Graphene Oxide Sheath on Ag Nanoparticle/Graphene Hybrid Films as an Antioxidative Coating and Enhancer of Surface-Enhanced Raman Scattering

Young-Kwan Kim,[†] Sang Woo Han,*,[†] and Dal-Hee Min*,[‡]

[‡]Department of Chemistry, Seoul National University, Seoul, 151-747, Republic of Korea
[†]Department of Chemistry and KI for the NanoCentury, KAIST, Daejeon, 305-701, Republic of Korea

Ⓢ Supporting Information

ABSTRACT: Surface-enhanced Raman scattering (SERS) has been extensively investigated since its discovery on rough Ag surface because of high sensitivity and resolution. Ag nanostructures are considered highly active for SERS but their liability to oxidization impedes their practical applications as a SERS-based sensing platform. Here, we show that graphene oxide (GO) coating on the polyallylamine hydrochloride (PAA) functionalized Ag nanoparticles (PAA-AgNP) immobilized on PAA-functionalized reduced GO (PAA-RGO) films (GO/PAA-AgNP/PAA-RGO, sandwich structure) protect AgNPs from oxidation under ambient condition for prolonged time up to 72 days with increased and reproducible SERS signals and fast adsorption kinetics of rhodamine 6G, a model Raman probe molecule. The present strategy for GO coating on top of the immobilized AgNPs will be useful for the development of an efficient SERS-based chemical and biosensor because of its simplicity, cost-effectiveness, long-term stability, and high reproducibility.

KEYWORDS: graphene oxide, protective coating, silver nanoparticle, surface enhanced Raman scattering, surface functionalization

GO/PAA-AgNP/PAA-RGO films

Long lasting SERS due to protection from oxidation

GO
AgNP
RGO
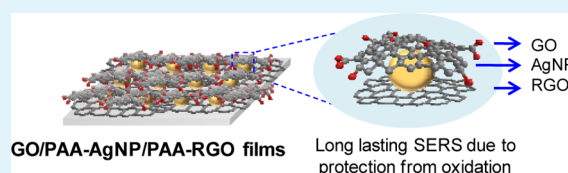
Since the discovery of huge Raman signal enhancement on the rough silver electrode surface in 1974,[1] surface enhanced Raman scattering (SERS) has attracted much attention because of high sensitivity for the analysis of various molecules at low concentrations. On the basis of the high sensitivity, the SERS has been widely demonstrated for chemical- and biosensors and bioimaging probes.[2] Thus, Ag and Au nanostructures with different morphologies have been investigated to develop efficient SERS platform but many challenges still remain.[3] For example, Ag is highly active metal as SERS platforms compared to Au but not an ideal candidate as itself for practical applications because of its liability to oxidation under ambient condition.[4] Moreover, colloidal stability of Ag nanoparticle (AgNP) is not sufficient to develop reproducible SERS platform. Therefore, many efforts have been devoted to fabricate stable Ag nanocomposites to avoid oxidation and aggregation by coating with titania,[5] silica,[6] and carbon shell.[7] The required properties as a coating shell of AgNP are ultrathin thickness (<10 nm), chemical inertness and reproducible synthetic or coating process. In this regard, the popular sol−gel method for the formation of titania and silica shell is not ideal because of difficulty in controlling reaction conditions to obtain well-defined shell thickness with high reproducibility. In contrast, carbon shell synthesized by chemical vapor deposition (CVD) and high-temperature carbonization is quite attractive because of chemical inertness and controllable thickness by adjusting CVD condition[8] and thickness of carbon layer before carbonization.[9] However, the processes to synthesize carbon shell require expensive equip-

ment and high-temperature treatment and thus, the development of simple and cost-effective strategy for the formation of carbon shell is still needed for various applications.

Graphene, a single layer of sp^2 carbon network arranged in a perfect honeycomb lattice, has been extensively investigated because of its excellent mechanical and electrical properties.[10,11] Recently, graphene oxide (GO), oxidized form of graphene, has attracted much attention because of its distinct physical properties such as water dispersibility, fluorescence, nonlinear optical absorption, and SERS.[12,13] The distinct properties are derived from its unique chemical structure composed of segregated sp^2 carbon domains among sp^3 carbons presenting various oxygen containing functional groups.[14] GO can be converted to reduced GO (RGO) by chemical and thermal treatment to increase sp^2 carbon domains.[15] To improve and endow new functions, metal and semiconductor NPs have been incorporated on RGO surface[16,17] and the resulting nanocomposites have been successfully harnessed as electrochemical[18,19] and photocatalyst,[20] biosensor,[21−24] energy device,[25] and SERS platform.[26,27] Especially, SERS on AgNP/RGO nanocomposites has been actively investigated because of amenable surface, large surface area, and high SERS activity. AgNP/RGO-based nanocomposites have been synthesized both in solution phase[28] and on solid substrates.[29] Although those efforts showed successful demonstration in the improve-

Scheme 1. Fabrication Process of GO/PAA-AgNP/PAA-RGO Films for Application as SERS Platform
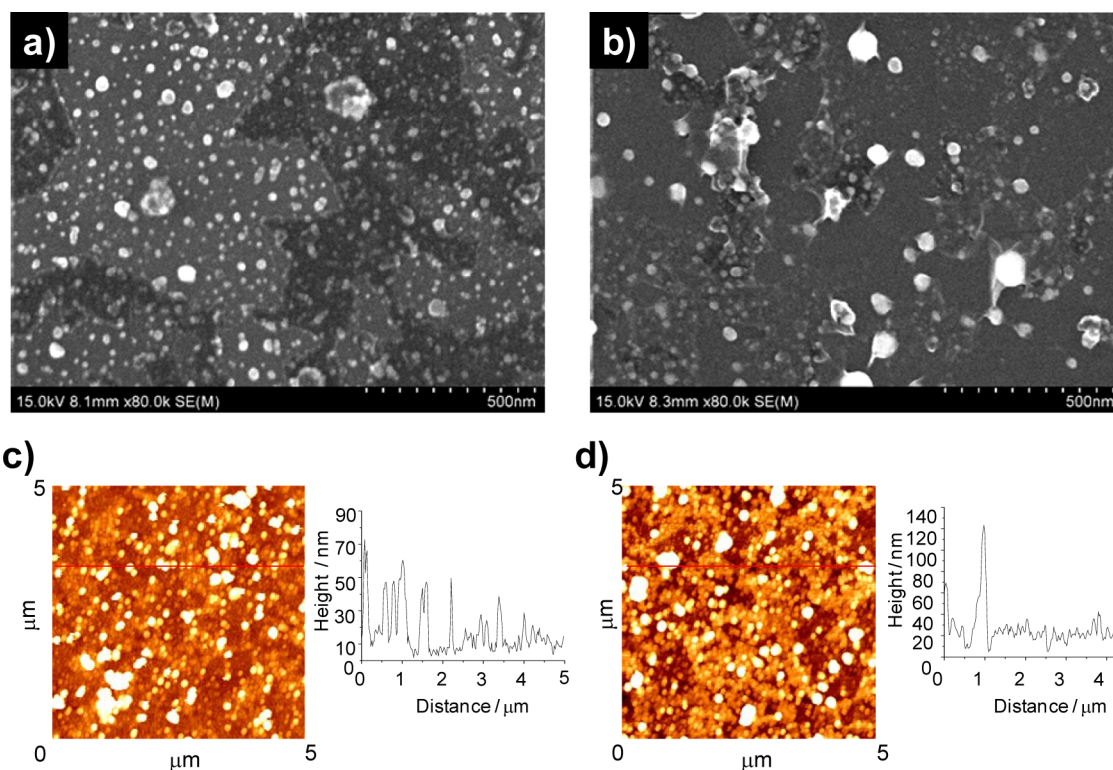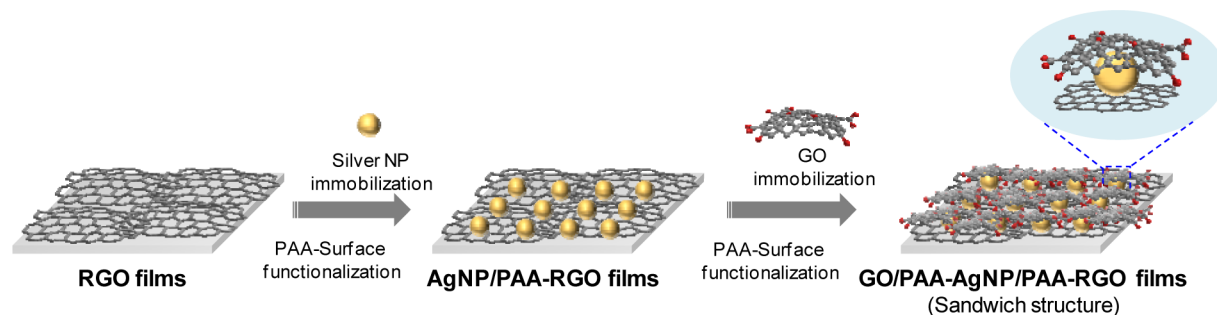

Figure 1. (a) SEM images of AgNP/PAA-RGO films and (b) GO/PAA-AgNP/PAA-RGO films. (c) AFM images and line profiles of AgNP/PAA-RGO films and (d) GO/PAA-AgNP/PAA-RGO films.

ment of the stability and reproducibility of SERS signal on AgNP, the instability of AgNP to oxidation under ambient condition still remains an important issue.

In the present study, AgNP/RGO hybrid films protected by GO sheath were fabricated by electrostatic adsorption of AgNP on polyallylamine hydrochloride (PAA) functionalized RGO (PAA-RGO) films and subsequent electrostatic adsorption of GO sheets on the PAA functionalized AgNP/PAA-RGO films (GO/PAA-AgNP/PAA-RGO, sandwich structure) to further enhance SERS signal intensity and protect AgNP from oxidation at the same time (Scheme 1). As a protective sheath on AgNP/PAA-RGO hybrid films, GO possesses several important features. First, the thickness of GO is about 1 nm.[26] The thin thickness of coating layer for SERS is important because thick coating (>10 nm) impedes SERS enhancement from AgNP.[6] Second, GO alone was shown as a favorable SERS platform, which therefore can serve as an additional enhancer of SERS signals.[30] Third, GO has affinity toward aromatic compounds, which are important targets of SERS-based chemical sensors.[31,32] Fourth, the present GO coating process

is cost-effective and simple compared to conventional processes to produce graphitic coating layer such as CVD or high-temperature carbonization.[8,9]

■ RESULTS AND DISCUSSION

The fabrication of GO/PAA-AgNP/PAA-RGO hybrid films started with synthesis of GO by a modified Hummers method (for characterization of GO, see Figure S1 in the Supporting Information.).[33] The synthesized GO sheets were dispersed in water by sonication for 30 min and immobilized on Si substrates modified with 3-aminopropyltriethoxysilane (APTES) by electrostatic interaction between negatively charged GO surface and positively charged Si substrates (Figure S2a,c in the Supporting Information).[34] Then, the GO thin films formed on Si substrates were reduced by immersing into 20% DMF solution of hydrazine monohydrate at 80 °C for 24 h. After reduction, the surface of RGO films was still negatively charged because of residual oxygen containing functional groups (Figure S2b,d in the Supporting Information).[34] The negatively charged surface of RGO films was
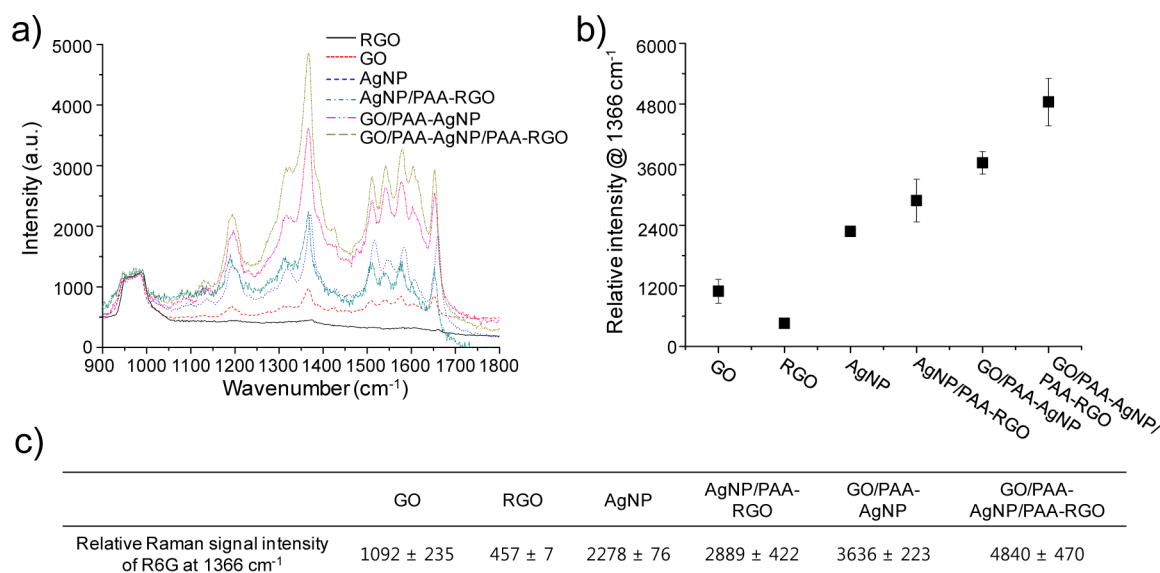
Figure 2. (a) Normalized SERS spectra and (b) relative Raman signal intensities of R6G obtained on GO, RGO, AgNP, AgNP/PAA-RGO, GO/PAA-AgNP, and GO/PAA-AgNP/PAA-RGO films. (c) Relative Raman signal intensities of R6G obtained on all of the prepared films. The error bars indicate the average and standard deviation of three measurements at different positions of the films.

modified with PAA to introduce amine groups and the PAA-RGO films were immersed in a freshly prepared colloidal solution of AgNP (∼25 nm in diameter) for 1 h to immobilize AgNP on the surface by electrostatic assembly.[35] The fabricated AgNP/PAA-RGO hybrid films were subsequently functionalized with PAA to induce positive charges on their surface. The PAA-AgNP/PAA-RGO hybrid films were then immersed into GO suspension (1 mg/mL) for 1 h for the formation of GO sheath on PAA-AgNP/PAA-RGO films by electrostatic interaction.[36]

Field-emission scanning electron microscopy (FE-SEM) image showed that the 25 nm-sized AgNP was densely immobilized on PAA-RGO films (Figure 1a), GO sheath was successfully assembled on the PAA-AgNP/PAA-RGO films and the AgNP on PAA-RGO films were clearly observed even after GO sheath formation because the GO layer was very thin (Figure 1b). To characterize the morphological changes of AgNP/PAA-RGO films by GO sheath formation, we analyzed the AgNP/PAA-RGO and GO/PAA-AgNP/PAA-RGO films by atomic force microscopy (AFM) and UV−vis spectroscopy. The AFM images of AgNP/PAA-RGO and GO/PAA-AgNP/PAA-RGO films showed similar morphology with their SEM images but it was difficult to directly observe the formation of GO sheath because AgNP was densely immobilized and partially aggregated (Figure 1c, d). However, the center line average (CLA) roughness of AgNP/PAA-RGO films (12.89) decreased to 12.43 despite of formation of many aggregated domains by GO sheath formation. The UV-spectrum of RGO films showed typical π−π* transition peak of aromatic C−C bond at 265 nm and the AgNP/PAA-RGO films showed an additional SPR band of AgNP at 387 nm, which was not shifted even after subsequent PAA-functionalization. After formation of GO sheath on PAA-AgNP/PAA-RGO films, the GO/PAA-AgNP/PAA-RGO films showed strong absorption peak at 252 nm from π−π* transition of GO sheath with shorter π-conjugation length than RGO and red-shift of SPR band from 387 to 393 nm by GO sheath-induced aggregation of AgNPs (Figure S3 in the Supporting Information). In addition to the morphological and spectroscopic changes, the chemical

composition change of AgNP/PAA-RGO films induced by GO sheath formation was confirmed by X-ray photoelectron spectroscopy (XPS). The C 1s XPS spectra of AgNP/PAA-RGO films showed typical peaks at 284.5, 286.0, 287.2, and 288.8 eV from graphitic C−C, C−O, C=O, and O−C=O bonds, respectively (see Figure S4a in the Supporting Information).[34] After GO sheath formation, the peak intensities at 286.0, 287.2, and 288.8 eV increased because more oxygen containing functional groups were introduced by adsorption of GO sheets on PAA-AgNP/PAA-RGO films (Figure S4b in the Supporting Information). These results indicate the successful formation of GO sheath on PAA-AgNP/PAA-RGO films.

Next, to investigate the effect of the RGO films underneath AgNP and the GO coating on top of the AgNP, we obtained the Raman spectra of rhodamine 6G (R6G) on six different films on Si substrates composed of GO, RGO, AgNP, AgNP/PAA-RGO, GO/PAA-AgNP, or GO/PAA-AgNP/PAA-RGO films after immersion of each substrate in 1 mM aqueous solution of R6G for 12 h to induce surface adsorption. The representative Raman spectra are shown in the Figure 2a and the relative Raman signal intensities of R6G at 1366 cm^{-1} were summarized in a table, Figure 2c (for all spectra, see Figure S5 in the Supporting Information). First, Raman signals of R6G on the AgNP, GO and RGO films were analyzed. Notable Raman signal enhancement of R6G was observed from GO and AgNP films. It is well-known that the Raman signal of aromatic compounds is enhanced on the surface of GO films by chemical enhancement[30] and on the AgNP immobilized surface by the formation of hot-spots.[37] However, RGO films showed little effect in the Raman signal enhancement of R6G compared to GO and AgNP films (Figure 2). This result is in good agreement with a previous report which demonstrates that the presence of oxygen containing functional groups in GO is one of the important reasons for Raman signal enhancement of the adsorbed molecules.[30]

Next, Raman signals of R6G from hybrid films including AgNP/PAA-RGO, GO/PAA-AgNP and GO/PAA-AgNP/PAA-RGO films were analyzed. Relative Raman signal of R6G on AgNP/PAA-RGO films was increased by 1.27 fold
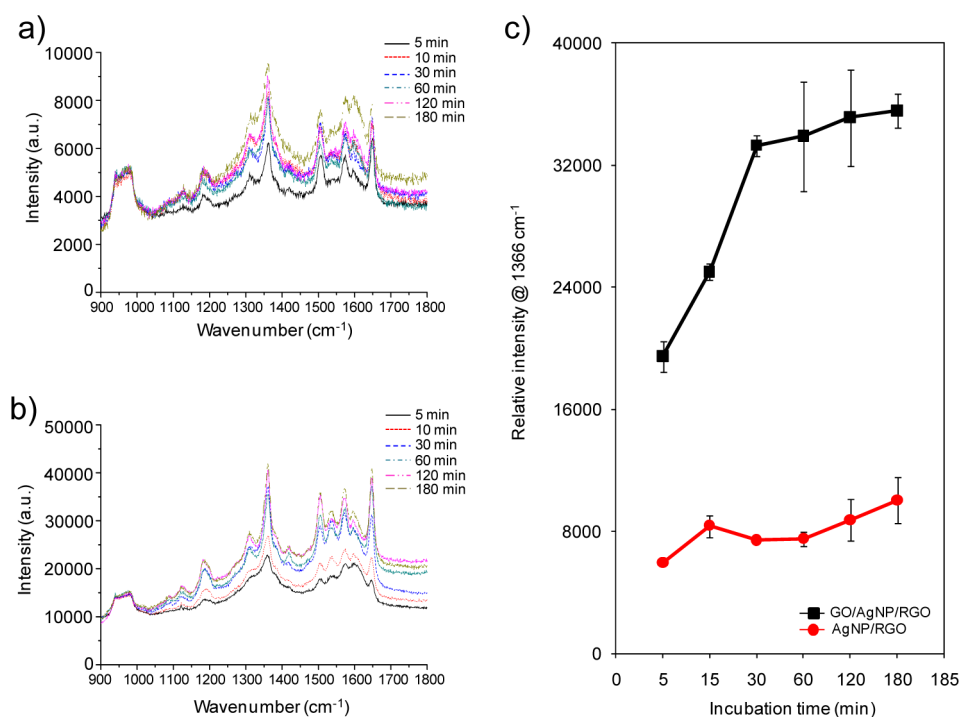
6547

dx.doi.org/10.1021/am301658p | ACS Appl. Mater. Interfaces 2012, 4, 6545−6551

Figure 3. (a) Normalized SERS spectra of R6G obtained on the AgNP/PAA-RGO films and (b) GO/PAA-AgNP/PAA-RGO films with varying incubation time for adsorption in 1 mM aqueous R6G. (c) A plot of normalized SERS signal intensities of R6G at 1366 cm^{-1} on AgNP/PAA-RGO and GO/PAA-AgNP/PAA-RGO films versus incubation time. Raman signal of R6G on GO/PAA-AgNP/PAA-RGO films was saturated at 30 min but that on AgNP/PAA-RGO films kept increasing even after 120 min of incubation time. The error bars indicate the average and standard deviation of 3 measurements at different positions of the films.

compared to that on AgNP films (Figure 2). It is well-known that the AgNP/RGO nanocomposites are more efficient SERS platform compared to AgNP alone, probably due to the aggregation of AgNPs on RGO surface (for characterization data of AgNP and AgNP/PAA-RGO films, see Figure S6 in the Supporting Information).[29] Then, the relative Raman signal intensity of R6G was further increased by 1.67 fold through the formation of GO sheath on the AgNP/PAA-RGO films (Figure 2). In addition, the relative Raman signal intensity of R6G at 1366 cm^{-1} on GO/PAA-AgNP/PAA-RGO films was 1.22 fold higher than the sum of relative Raman signal intensities of R6G obtained on GO and AgNP/PAA-RGO films (Figure 2). The GO sheath induced relative Raman signal increase was further confirmed by the formation of GO sheath on PAA-AgNP films. After formation of the GO sheath on PAA-AgNP films, the relative Raman signal intensity of R6G on AgNP films was increased by 1.60 fold, which was slightly higher than the relative Raman signal increase on GO/PAA-AgNP/PAA-RGO films relative to AgNP/PAA-RGO films (1.26 fold) (Figure 2). Interestingly, the relative Raman signal of R6G on GO/PAA-AgNP/PAA-RGO films was 1.33 fold higher than that on GO/PAA-AgNP films (Figure 2) and this relative Raman signal increase was also comparable to that on AgNP/PAA-RGO films compared to AgNP films (1.26 fold), which implied that both the PAA-RGO films underneath AgNP and the GO coating on the PAA-AgNP films contributed to the Raman signal increase in R6G.

Next, the influence of GO sheath on the adsorption kinetics of R6G was examined by measuring the changes of relative SERS signal intensity on both AgNP/PAA-RGO and GO/PAA-AgNP/PAA-RGO films as a function of incubation time of the respective hybrid films in 1 mM aqueous solution of R6G

allowed for adsorption. SERS signal of R6G on AgNP/PAA-RGO films increased gradually for 180 min (Figure 3a, c) but the increase in the SERS signal of R6G on GO/PAA-AgNP/PAA-RGO films was almost saturated after 30 min (Figure 3b, c). This result clearly indicated that the GO sheath accelerated the adsorption of R6G by the strong $\pi-\pi$ interaction.[31] Additionally, the AgNP/PAA-RGO and GO/PAA-AgNP/PAA-RGO films showed the high SERS activity with homogeneous Raman signal of R6G throughout the overall surface (Figure and Figure S7 in the Supporting Information). Taken together, the results confirmed that the formation of GO sheath and supporting RGO films significantly improved the SERS activity of AgNP films with homogeneous Raman signals on the entire surface and accelerated adsorption of R6G.

As a control, PAA-RGO films were applied to SERS analysis of R6G to investigate the influence of PAA used to immobilize AgNP on RGO films on SERS activity. PAA-RGO films did not give notable changes on SERS activity compared to RGO films (see Figure S8 in the Supporting Information). The results confirmed that PAA as an interlayer adhesive for the formation of GO/PAA-AgNP/PAA-RGO films exhibit little effect to the Raman signals of R6G on the GO/PAA-AgNP/PAA-RGO.

To investigate the protection effect of GO sheath on the PAA-AgNP/PAA-RGO film from oxidation of AgNP, the AgNP/PAA-RGO and the GO/PAA-AgNP/PAA-RGO films were prepared and exposed to ambient condition for designated durations of 0, 3, 13, and 72 days. Next, the AgNP/PAA-RGO and GO/PAA-AgNP/PAA-RGO films were respectively incubated in 1 mM aqueous solution of R6G for 12 h and analyzed by Raman spectroscopy. The relative Raman signal intensities of R6G at 1366 cm^{-1} derived from aromatic C−C stretching modes on freshly prepared AgNP/PAA-RGO and
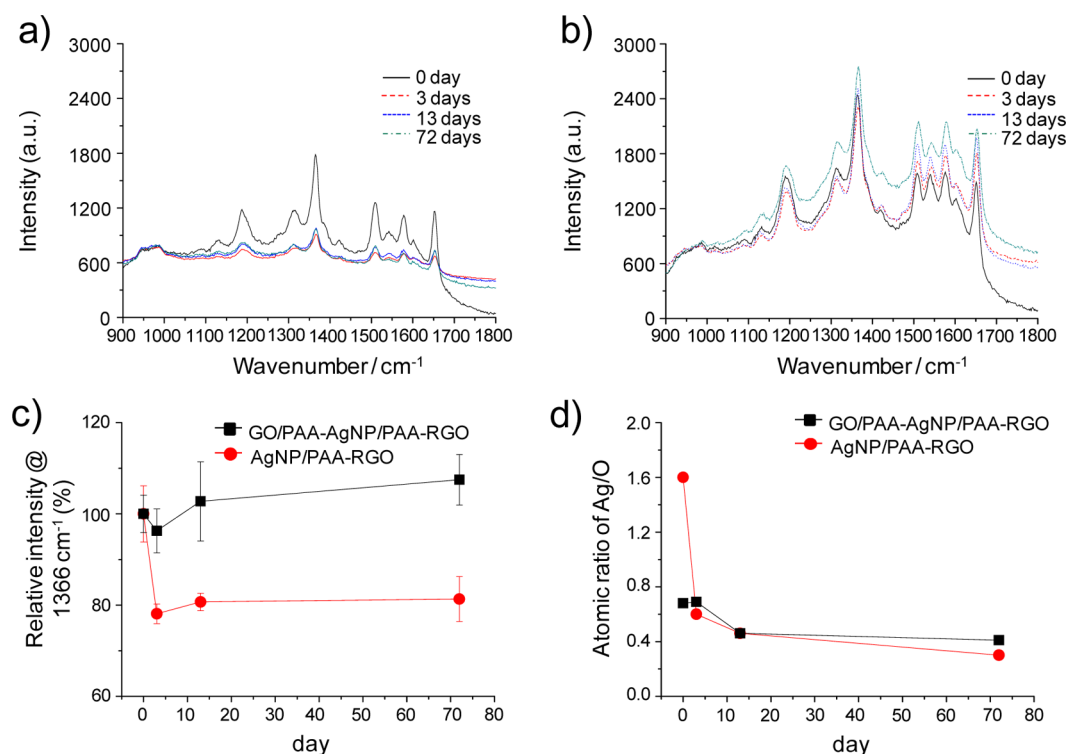
Figure 4. (a) Normalized SERS spectra of R6G obtained on the AgNP/PAA-RGO films and (b) GO/PAA-AgNP/PAA-RGO films after exposure to ambient condition for 0, 3, 13, and 72 days. (c) The plots of normalized SERS signal intensity at 1366 cm^{-1} on AgNP/PAA-RGO and GO/PAA-AgNP/PAA-RGO films, the error bars indicate the average and standard deviation of 5 measurements at different positions of the films, and (d) atomic ratio of Ag/O of AgNP/PAA-RGO and GO/PAA-AgNP/PAA-RGO films as a function of exposure time to ambient condition.

GO/PAA-AgNP/PAA-RGO films were obtained by averaging 5 point measurements, which provided a highly reproducible spectra (for all spectra, see Figure S9 in the Supporting Information). When AgNP/PAA-RGO and GO/PAA-AgNP/PAA-RGO films were applied to Raman analysis of R6G after 3 day exposure to ambient condition, the relative Raman signal intensity on AgNP/PAA-RGO films significantly decreased by 21.90 ± 2.2% but that on GO/PAA-AgNP/PAA-RGO films slightly decreased only by 3.62 ± 4.8% (Figure 4a–c). This result indicated that the enhanced Raman signal on GO/PAA-AgNP/PAA-RGO films was stable even after exposure to ambient condition compared to that on AgNP/PAA-RGO films. This tendency was maintained when the AgNP/PAA-RGO and GO/PAA-AgNP/PAA-RGO were employed for Raman analysis after 13 and 72 day exposure to ambient condition (Figure 4a,b,c). The relatively consistent enhanced Raman signals on GO/PAA-AgNP/PAA-RGO films can be attributed to the presence of GO sheath which protects AgNP on RGO films from oxidation.

To investigate the influence of the PAA-adhesive layer on AgNP protection from oxidation, AgNP/PAA-RGO, PAA-AgNP/PAA-RGO and GO/PAA-AgNP/PAA-RGO films were heated to 250 °C for 3, 5, 15, and 25 min under air to accelerate oxidation of AgNP without thermal degradation of PAA.[38] After oxidative treatment, those films were analyzed by UV−vis spectroscopy to monitor the red-shift and broadening of SPR band of AgNP induced by oxidation.[39] The SPR band of AgNP/PAA-RGO films at 372 nm was significantly broadened within 5 min oxidative treatment and this result suggested that the AgNPs on PAA-RGO films started to be oxidized within 5 min (see Figure S10a in the Supporting Information). By contrast, the SPR band of PAA-AgNP/PAA-RGO films was not

affected by 5 min oxidative treatment and only slightly broadened by further oxidative treatment up to 25 min (see Figure S10b in the Supporting Information). This result clearly indicated that the PAA-adhesive layer contributed to the protection of AgNP from oxidation. In comparison with those two films, the changes of SPR band of GO/PAA-AgNP/RGO films could not be directly correlated with oxidation of AgNP because the thermal treatment could result in the reduction of GO sheath with increased absorption in visible region,[40] which could induce changes in the SPR band without oxidation of AgNP. Actually, the SPR band of GO/PAA-AgNP/PAA-RGO films was red-shifted from 400 to 415 nm by only 3 min oxidative treatment (see Figure S10c in the Supporting Information) but this red-shift could be attributed to GO sheath reduction because the SPR band of AgNP without protective layer was not changed by the same oxidative treatment (see Figure S10a in the Supporting Information). Moreover, the SPR band of GO/PAA-AgNP/PAA-RGO films was not further red-shifted by oxidative treatment up to 25 min despite of the significant increase of absorption in visible region (see Figure S10c in the Supporting Information). These results clearly indicated that the sustained SERS activity of GO/PAA-AgNP/PAA-RGO films was originated from the cooperative protection effect of PAA-adhesive layer and GO sheath.

To further investigate the protection of AgNP by PAA-adhesive layer and GO sheath, the AgNP/PAA-RGO and GO/PAA-AgNP/PAA-RGO films exposed to designated periods of 0, 3, 13, and 72 days to ambient condition were analyzed by X-ray photoelectron spectroscopy (XPS) to reveal the changes in the chemical composition of each hybrid film over time. The Ag/O ratio of AgNP/PAA-RGO and GO/PAA-AgNP/PAA-RGO films was plotted versus exposure time. The initial Ag/O

ratio of AgNP/PAA-RGO and GO/PAA-AgNP/PAA-RGO films was respectively 1.60 and 0.68 but those values decreased to 0.30 and 0.41 after 72 day exposure to ambient condition (see Figure 4d and Figure S11 in the Supporting Information). The different initial Ag/O ratio of AgNP/PAA-RGO with GO/PAA-AgNP/PAA-RGO films was due to the presence of GO sheath, which increased the oxygen content of the GO/PAA-AgNP/PAA-RGO films compared to AgNP/PAA-RGO films (see Figure S3b in the Supporting Information). The decrease in the Ag/O ratio over time implies that the AgNP incorporated in those hybrid films was oxidized. The decrease in Ag/O ratio was more significant on AgNP/PAA-RGO films compared to GO/PAA-AgNP/PAA-RGO films. These data confirm that the consistent SERS performance of GO/PAA-AgNP/PAA-RGO films was derived from the protection of AgNP/PAA-RGO films from oxidation by GO sheath.

CONCLUSION

We developed a strategy for the coating of AgNP/PAA-RGO films by GO sheets with PAA-adhesive layer through electrostatic assembly both for the enhancement of Raman signals and for the prevention of the oxidation of AgNP incorporated in the hybrid films upon exposure to ambient condition for prolonged time. The Raman signal of R6G on AgNP/PAA-RGO films was enhanced by 1.67 fold and adsorption process of the analyte molecule was at least 6 fold faster through the formation of GO sheath on their surface. Most importantly, the GO sheath protected AgNP/PAA-RGO films from oxidation under ambient condition for prolonged time up to 72 days. As a result, the developed GO/PAA-AgNP/PAA-RGO films showed the enhanced and reproducible Raman signal of R6G even after prolonged exposure to ambient condition. The present strategy to form GO sheath on AgNP/PAA-RGO films is a simple approach to fabricate the ultrathin graphitic coating layer on surface-immobilized AgNP films without using any expensive equipment or high temperature processes. We believe that the present strategy could be a useful and convenient route to prepare robust and reproducible SERS platform for efficient SERS-based chemical and biosensing.

MATERIALS AND METHODS

Materials. Natural graphite (FP 99.95% pure) was purchased from Graphit Kropfmühl AG (Hauzenberg, Germany). Sodium nitrate, sodium sulfate, hydrazine monohydrate, trisodium citrate dehydrate and hydrogen peroxide (30% in water) were purchased from Junsei (Japan). Potassium permanganate, poly(allylamine hydrochloride) (PAA) (MW 15,000), 3-aminopropyltriethoxysilane (APTES), sodium borohydride, anhydrous toluene, and silver nitrate were purchased from Aldrich Chemical Co. (Milwaukee, WI, USA). Nitric acid and sulfuric acid were purchased from Samchun (Seoul, Korea). Ethanol was purchased from Merck (Darmstadt, Germany). Si substrates (500 μm in thickness) were purchased from STC (Japan). All chemicals were used as received.

Preparation of GO. Three g of natural graphite and 1 g of sodium nitrate were added to 46 mL of sulfuric acid and stirred in an ice bath. Six grams of potassium permanganate was gradually added to the mixture with stirring and maintained below 20 °C. After the addition, the temperature of the mixture was raised to 35 °C and the mixture was further stirred for an hour. 40 mL of water was slowly added to the mixture, stirred for 30 min and diluted with 100 mL of water in an ice bath to prevent rapid boiling because this process causes rapid increase of temperature. Finally, 6 mL of hydrogen peroxide (30%) was gradually added to the mixture with color change to bright yellow and formation of bubbles. The final mixture was filtered with filter paper (Number 3, Whatman) and washed with water until the filtrate was

neutralized. The filtered solid was dried under reduced pressure for 48 h.

Preparation of APTES-Modified Glass Substrates. The Si substrates were cleaned in Piranha solution (sulfuric acid: hydrogen peroxide (30%) = 3:1, WARNING: Piranha solution is extremely explosive and corrosive.) for 10 min at 125 °C, washed with water and ethanol, and dried under a stream of nitrogen. The substrates were immersed in a 10 mM anhydrous toluene solution of APTES for 30 min, briefly sonicated in toluene for 2 min, rinsed with ethanol and water, and dried under a stream of nitrogen.

Prepration of GO, RGO, AgNP, AgNP/PAA-RGO, GO/PAA-AgNP, and GO/AgNP/RGO Films. For formation of GO films, APTES-treated Si substrates were immersed in the GO suspension (1 mg/mL) for 1 h, washed with water and ethanol, dried under a stream of nitrogen and baked at 150 °C under nitrogen flow. For preparation of RGO films, GO films coated substrates were reduced by immersing in hydrazine monohydrate solution (20% in N,N-dimethylformamide (DMF)) for 24 h at 80 °C; washed with DMF, water, and ethanol; and dried under a stream of nitrogen. For preparation of AgNP films, piranha treated Si substrates were immersed in aqueous PAA solution (1 mg/mL, pH 7.5) for 30 min, washed with water and ethanol, and dried under a stream of nitrogen. The PAA-treated Si substrates were incubated with AgNP solution for 1 h, washed with water and ethanol, and dried under a stream of nitrogen. For preparation of AgNP/PAA-RGO films, PAA-treated RGO films coated substrates were incubated with AgNP solution for 1 h, washed with water and ethanol, and dried under a stream of nitrogen. For preparation of GO/PAA-AgNP films, PAA treated AgNP films were immersed in the GO suspension for 1 h, washed with water and ethanol and dried under a stream of nitrogen. For preparation of GO/PAA-AgNP/PAA-RGO films, PAA-treated AgNP/RGO films coated substrates were immersed in GO suspension for 1 h, washed with water and ethanol, and dried under a stream of nitrogen.

Confirmation of Protection Effect of GO Sheath. Two sets of AgNP/PAA-RGO and GO/PAA-AgNP/PAA-RGO films coated substrates were prepared and exposed to ambient condition for certain times such as 0, 3, 13, and 72 days. After exposure, one set of AgNP/PAA-RGO and GO/PAA-AgNP/PAA-RGO films coated substrates were analyzed by XPS to reveal their chemical composition changes and the other set was immersed in 1 mM aqueous solution of rhodamine 6G for 12 h, washed with water and ethanol, dried under a stream of nitrogen, and analyzed by Raman spectroscopy to investigate the influence of GO sheath on SERS performance after prolonged exposure to ambient condition.

Characterization. The surface morphologies of AgNP/PAA-RGO and GO/PAA-AgNP/PAA-RGO films were observed by S-4800 FE-SEM (Hitach, Japan). Atomic force microscopy (AFM) images, line-profiles and center-line average surface roughness of prepared substrates were obtained with an XE-100 (Park System, Korea) with a backside gold-coated silicon SPM probe (M to N, Korea). High-resolution XPS measurements were carried out with an SIGMA PROBE (ThermoVG, U.K) with monochromatic Al−K (1.5 kV). The UV−vis spectra were recorded with a UV-2550 (Shimadzu, Japan). Raman characterization was carried out by LabRAM HR UV/vis/NIR (Horiba Jobin Yvon, France) using an 20 mW Ar ion CW laser (514.5 nm) as an excitation source focused through a BXFM confocal microscope equipped with an objective (50×, numerical aperture = 0.50). Raman signal intensity of rhodamine 6G was normalized by using a silicon peak at ~1000 cm^{-1} as an internal standard. FT-IR spectra measurements of graphite oxide were performed with an EQUINOX55 (Bruker, Germany) using the KBr pellet method.

ASSOCIATED CONTENT

Ⓢ Supporting Information

Additional figures of analytical data. This material is available free of charge via the Internet at http://pubs.acs.org.

■ AUTHOR INFORMATION

Corresponding Author

*Fax: +82-42-350-2810 (S.W.); +82-2-889-1568 (D.-H.M.). Tel: +82-42-350-2812 (S.W.); +82-2-880-4338 (D.-H.M.). E-mail: sangwoohan@kaist.ac.kr (S.W.); dalheemin@snu.ac.kr (D.-H.M.).

Notes

The authors declare no competing financial interest.

■ REFERENCES

(1) Fleischmann, M.; Hendra, P. J.; McQuillan, A. J. *Chem. Phys. Lett.* **1974**, *26*, 163−166.

(2) Alvarez-Puebla, R. A.; Liz-Marzán, L. M. *Small* **2010**, *6*, 604−10.

(3) Henry, A. I.; Bingham, J. M.; Ringe, E.; Marks, L. D.; Schatz, G. C.; Van Duyne, R. P. *J. Phys. Chem. C* **2011**, *115*, 9291−9305.

(4) Han, Y.; Lupitskyy, R.; Chou, T. M.; Stafford, C. M.; Du, H.; Sukhishvili, S. *Anal. Chem.* **2011**, *83*, 5873−5880.

(5) Bao, L.; Mahurin, S. M.; Dai, S. *Anal. Chem.* **2004**, *76*, 4531−4536.

(6) Li, J. F.; Huang, Y. F.; Ding, Y.; Yang, Z. L.; Li, S. B.; Zhou, X. S.; Fan, F. R.; Zhang, W.; Zhou, Z. Y.; Wu, D. Y.; Ren, B.; Wang, Z. L.; Tian, Z. Q. *Nature* **2010**, *464*, 392−395.

(7) Chen, L. M.; Liu, Y. N. *ACS Appl. Mater. Interfaces* **2011**, *3*, 3091−3096.

(8) Chen, S.; Brown, L.; Levendorf, M.; Cai, W.; Ju, S. Y.; Edgeworth, J.; Li, X.; Magnuson, C. W.; Velamakanni, A.; Piner, R. D.; Kang, J.; Park, J.; Ruoff, R. S. *ACS Nano* **2011**, *5*, 1321−1327.

(9) Yang, D.; Xia, L.; Zhao, H.; Hu, X.; Liu, Y.; Li, J.; Wan, X. *Chem. Commun.* **2011**, *47*, 5873−5875.

(10) Geim, A. K.; Novoselov, K. S. *Nat. Mater.* **2007**, *6*, 183−191.

(11) He, Q.; Wu, S.; Yin, Z.; Zhang, H. *Chem. Sci.* **2012**, *3*, 1764−1772.

(12) Loh, K. P.; Bao, Q.; Eda, G.; Chhowalla, M. *Nat. Chem.* **2010**, *2*, 1015−1024.

(13) Qi, X.; Li, H.; Lam, J. W.; Yuan, X.; Wei, J.; Tang, B. Z.; Zhang, H. *Adv. Mater.* **2012**, *24*, 4191−4195.

(14) Bagri, A.; Mattevi, C.; Acik, M.; Chabal, Y. J.; Chhowalla, M.; Shenoy, V. B. *Nat. Chem.* **2010**, *2*, 581−587.

(15) Stankovich, S.; Dikin, D. A.; Dommett, G. H.; Kohlhaas, K. M.; Zimney, E. J.; Stach, E. A.; Piner, R. D.; Nguyen, S. T.; Ruoff, R. S. *Nature* **2006**, *442*, 282−286.

(16) Huang, X.; Qi, X.; Boey, F.; Zhang, H. *Chem. Soc. Rev.* **2012**, *41*, 666−686.

(17) Huang, X.; Yin, Z.; Wu, S.; Qi, X.; He, Q.; Zhang, Q.; Yan, Q.; Boey, F.; Zhang, H. *Small* **2011**, *7*, 1876−1902.

(18) Liang, Y.; Li, Y.; Wang, H.; Zhou, J.; Wang, J.; Regier, T.; Dai, H. *Nat. Mater.* **2011**, *10*, 780−786.

(19) Wang, Z.; Zhang, J.; Yin, Z.; Wu, S.; Mandler, D.; Zhang, H. *Nanoscale* **2012**, *4*, 2728−2733.

(20) Zhang, H.; Lv, X.; Li, Y.; Wang, Y.; Li, J. *ACS Nano* **2010**, *4*, 380−386.

(21) Li, L. L.; Liu, K. P.; Yang, G. H.; Wang, C. M.; Zhang, J. R.; Zhu, J. J. *Adv. Funct. Mater.* **2011**, *21*, 869−878.

(22) Yin, Z.; He, Q.; Huang, X.; Zhang, J.; Wu, S.; Chen, P.; Lu, G.; Chen, P.; Zhang, Q.; Yan, Q.; Zhang, H. *Nanoscale* **2012**, *4*, 293−297.

(23) Lu, G.; Li, H.; Liusman, C.; Yin, Z.; Wu, S.; Zhang, H. *Chem. Sci.* **2011**, *2*, 1817−1821.

(24) Chen, P.; Yin, Z.; Huang, X.; Wu, S.; Liedberg, B.; Zhang, H. *J. Phys. Chem. C* **2011**, *115*, 24080−24084.

(25) Yang, N.; Zhai, J.; Wang, D.; Chen, Y.; Jiang, L. *ACS Nano* **2010**, *4*, 887−894.

(26) Kim, Y.-K.; Na, H.-K.; Lee, Y. W.; Jang, H.; Han, S. W.; Min, D.-H. *Chem. Commun.* **2010**, *46*, 3185−3187.

(27) Kim, Y.-K.; Na, H.-K.; Min, D. H. *Langmuir* **2010**, *26*, 13065−13070.

(28) Tang, X. Z.; Cao, Z.; Zhang, H. B.; Liu, J.; Yu, Z. Z. *Chem. Commun.* **2011**, *47*, 3084−3086.

(29) Zhou, X.; Huang, X.; Qi, X.; Wu, S.; Xue, C.; Boey, F. Y. C.; Yan, Q.; Chen, P.; Zhang, H. *J. Phys. Chem. C* **2009**, *113*, 10842−10846.

(30) Yu, X.; Cai, H.; Zhang, W.; Li, X.; Pan, N.; Luo, Y.; Wang, X.; Hou, J. G. *ACS Nano* **2011**, *5*, 952−958.

(31) Liu, X.; Cao, L.; Song, W.; Ai, K.; Lu, L. *ACS Appl. Mater. Interfaces* **2011**, *3*, 2944−2952.

(32) Gao, W.; Majumder, M.; Alemany, L. B.; Narayanan, T. N.; Ibarra, M. A.; Pradhan, B. K.; Ajayan, P. M. *ACS Appl. Mater. Interfaces* **2011**, *3*, 1821−1826.

(33) Hummers, W. S.; Offeman, R. E. *J. Am. Chem. Soc.* **1958**, *80*, 1339.

(34) Kim, Y.-K.; Min, D.-H. *Langmuir* **2009**, *25*, 11302−11306.

(35) Kim, Y.-K.; Min, D. -H. *Langmuir* **2012**, *28*, 4453−4458.

(36) The assembly of chemically functionalized GO sheets on AgNP immobilized surface was previously reported by Lu and co-workers. In the report, the surface of GO sheets was functionalized by 3-mercaptopropyltrimethoxysilane (MPTMS) to introduce free thiol groups for the immobilization of GO sheets on AgNP films and the resulting GO coated Ag films showed high affinity to various aromatic compound such as crystal violet (CV) with positive charge, amaranth with negative charge, and neutral phosphorus triphenyl (PPh_3) for SERS detection.[31] However, the protective effect of GO sheath coating on AgNP films has not been explored yet. In addition, the surface of GO sheets used in the present study was not chemically functionalized unlike their approach, and therefore, could provide simpler GO sheath preparation process and relatively higher affinity to aromatic compounds compared to the MPTMS functionalized GO sheets.

(37) Freeman, R. G.; Grabar, K. C.; Allison, K. J.; Bright, R. M.; Davis, J. A.; Guthrie, A. P.; Hommer, M. B.; Jackson, M. A.; Smith, P. C.; Walter, D. G.; Natan, M. J. *Science* **1995**, *267*, 1629−1632.

(38) Hu, J.; He, Bo.; Lu, J.; Hong, L.; Yuan, J.; Song, J.; Niu, L. *Int. J. Electrochem. Sci.* **2012**, *7*, 10094−10107.

(39) Lok, C. N.; Ho, C. M.; Chen, R.; He, Q. Y.; Yu, W. Y.; Sun, H.; Tam, P. K.; Chiu, J. F.; Che, C. M. *J. Biol. Inorg. Chem.* **2007**, *12*, 527−534.

(40) Zangmeister, C. D. *Chem. Mater.* **2010**, *22*, 5625−5629.

6551

dx.doi.org/10.1021/am301658p | *ACS Appl. Mater. Interfaces* 2012, 4, 6545−6551